Computer Simulation Studies of Molecular Orientation in Polyethylene Networks: Orientation Functions and the Legendre Addition Theorem†

J. I. Cail, D. J. R. Taylor, and R. F. T. Stepto*

Polymer Science & Technology Group, Manchester Materials Science Centre, UMIST & University of Manchester, Grosvenor Street, Manchester, M1 7HS U.K.

M. G. Brereton, R. A. Jones, M. E. Ries, and I. M. Ward

IRC in Polymer Science & Technology, Department of Physics, University of Leeds, Leeds, LS2 9JT U.K.

Received November 16, 1999; Revised Manuscript Received March 30, 2000

ABSTRACT: Correction of an averaging procedure used previously to evaluate, from Monte Carlo calculations, $\langle P_2(\zeta)\rangle$, the mean orientation function of segments with respect to the direction of uniaxial macroscopic strain in polyethylene networks, is described. The correction takes into account the interdependence of segment orientation and chain orientation as chains become more extended and aligned under uniaxial stress. Segment orientation soon becomes nonrandom, and the corrected values of $\langle P_2(\zeta)\rangle$ show significant nonlinear behavior even near deformation ratio $\lambda = 1$, with respect to normalized stress versus $\lambda^2 - \lambda^{-1}$. It is demonstrated that such behavior leads to stress−orientation coefficients (Z_t) deduced from experimental stress−optical coefficients (C_{expt}) being larger than the true, limiting values as $\lambda \rightarrow 1$. Correction of the experimentally derived values of Z_t leads to agreement between theory and experiment being achieved for polyethylene on the basis the value of $\Delta\tilde{n}_{max}$, the maximum segmental birefringence in polyethylene chains, derived using Denbigh's estimates of bond polarizabilities.

Introduction

In a recent publication,[1] segmental orientation in polyethylene (PE) networks was investigated using a Monte Carlo (M−C) model to evaluate the contributions to the overall segmental orientation from individual network chains. The first stage in the modeling procedure involved the detailed calculation, using a rotational isomeric state (RIS) approach, of the average segment angle, ξ, relative to the chain end-to-end vector (**r**), for an individual, unperturbed PE chain as a function of chain extension. For each conformation sampled using the M−C scheme, the orientations of individual $-CH_2-$ segment vectors, relative to the chain vector, were calculated. The segment vector, shown in Figure 1a, is defined as the vector passing through the skeletal C atom in a direction parallel to the chain axis of an all-trans chain. More specifically, the vector for the ith segment lies in the plane of the ith and $(i-1)$th skeletal bonds and at 34° to both bonds (since the C−C−C valence angle supplement $\theta = 68°$ for PE[2]). Therefore, a chain of $n + 1$ segments (n skeletal bonds) was described in terms of $n - 1$ segment vectors ($i = 2$ to $i = n$), and the average bond orientation for a given magnitude of end-to-end distance (r) was expressed using the average orientation function, $\langle P_2(\xi)\rangle = {}^1/_2(3\langle\cos^2\xi\rangle - 1)$.

The network was subsequently represented by an array of individual PE chains, initially randomly oriented in three dimensions. This model network was deformed uniaxially, and assuming affine deformation of network chains up to their maximum extensions,[1,3,4] the resulting changes in the $\langle P_2(\xi)\rangle$ function for each chain, i, were calculated to give $\langle P_2(\xi)\rangle_i$. The associated changes in end-to-end vector orientation relative to the uniaxial strain direction, ψ, and hence the orientation

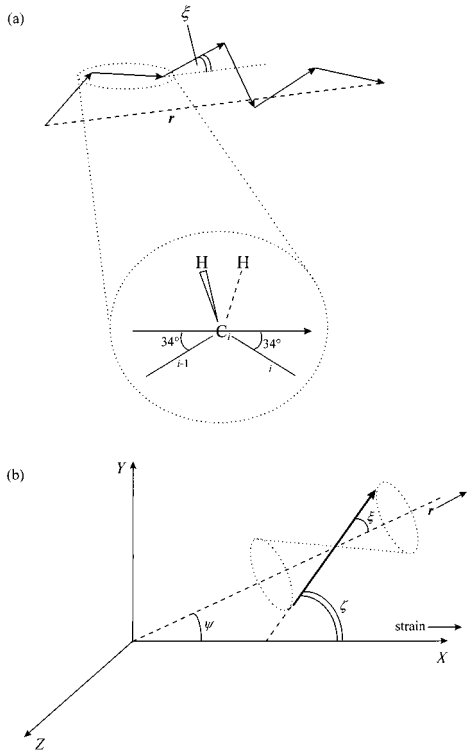

Figure 1. (a) Illustration of the orientation angle ξ between a segment vector and the chain vector, **r**. (b) Illustration of orientation angles: ξ, between a segment vector and chain vector, **r**; ψ, between **r** and the uniaxial strain direction; and ζ, the effective angle between a segment vector and the strain direction. The segment is assumed to randomly occupy all positions on the cone defined by ξ, so that the calculated value of $P_2(\zeta)$ is an average, sampled over all cone positions of ξ.

† Dedicated with best wishes to Karel Dušek on the occasion of his 70th birthday.

* To whom correspondence should be addressed.

10.1021/ma991943n CCC: $19.00
Published on Web 05/20/2000

function, $P_2(\psi)$, were also calculated (see Figure 1b). The average bond orientation, $\langle P_2(\zeta)\rangle$, over all chains i in the M−C sample, *relative to the uniaxial strain direction*, was calculated using the limiting approximation[1]

$$\langle P_2(\zeta)\rangle = \langle\langle P_2(\xi)\rangle_i\rangle\langle P_2(\psi_i)\rangle \quad (1)$$

Thus, it was assumed that the average orientation functions $\langle\langle P_2(\xi)\rangle_i\rangle$ and $\langle P_2(\psi_i)\rangle$, over the M−C sample of i chains, are independent. This is only strictly true in the zero-deformation limit ($\lambda \rightarrow 1$). The correct use of the Legendre addition theorem requires that the average product

$$\langle P_2(\zeta)\rangle = \langle\langle P_2(\xi)\rangle_i P_2(\psi_i)\rangle \quad (2)$$

is formed, rather than the product of the averages.

The original series of network deformation calculations on polyethylene have now been repeated, with $\langle P_2(\zeta)\rangle$ evaluated using eq 2. The present paper reports the results obtained and compares them with those previously derived using eq 1 and with the experimental data previously considered.[1] Interesting differences in behavior and in the interpretation of the experimental data are found. The paper also considers the limiting stress−optical behavior of equivalent Gaussian chains.

Summary of the M−C Simulation of Network Stress−Strain and Orientational Behavior

The M−C algorithm described previously[3,4] was used to calculate the dimensions of individual PE chains of $n = 40-220$ skeletal bonds. The RIS parameters pertaining to the PE chain structure were those of Abe, Jernigan, and Flory.[2] M−C sample sizes of 3×10^6 chain conformations were used, and the calculated values of the mean-square end-to-end distance, $\langle r^2\rangle$, differed from their *exact* RIS values, calculated using matrix algebra,[5,6] by less than 0.1%.

Radial end-to-end distance distributions, $W(r)$, were formed as histograms, over the whole M−C samples of chain conformations. As discussed previously,[4] the M−C distributions show that conformations above a certain value of r (denoted r^*_{max}) occur with negligible probabilities (given that numbers are stored to six decimal places). Hence, in the M−C samples of up to 3×10^6 chains, the values of $P(\mathbf{r})$ at $r = r^*_{max}$ are extremely small, of the order of $10^{-5}-10^{-6}$ times the values at $r = 0$. For $r > r^*_{max}$, $W(r)$ is then effectively zero, and r^*_{max} is therefore the *effective conformationally* fully extended end-to-end distance of the real polymer chain. As the PE chain length is increased from 40 to 220 skeletal bonds, the ratio r^*_{max}/r_{max} decreases, where r_{max} is the end-to-end distance of the all-trans chain.

From $W(r)$, the corresponding probability density functions, $P(\mathbf{r})$, were calculated using

$$P(\mathbf{r}) = \frac{W(r)}{4\pi r^2} \quad (3)$$

assuming random orientation of the end-to-end vectors, $\mathbf{r}$, for undeformed chains. The elastic, Helmholtz free energy of a chain[3] is $-kT \ln P(\mathbf{r})$. $\ln P(\mathbf{r})$ was evaluated as a function of r/r_{max} and stored for use in the network deformation algorithm. For stress−optical calculations, $\langle P_2(\xi)\rangle$, the segmental orientation function averaged over all segments in a chain was also evaluated over the whole M−C samples of chain conformations as a function of r/r_{max}.

A network was constructed from a population of chains with end-to-end distances distributed according to $W(r)$ randomly oriented in external space. In the M−C network deformation algorithm a sample of $N \approx 5 \times 10^6$ individual chains was chosen randomly from the population and subjected to a range of uniaxial macroscopic deformation ratios, λ, in a fixed external direction. The deformation is affine up to $r = r^*_{max}$. Beyond that point, as $W(r \geq r^*_{max}) = 0$ and no conformations occur, a chain vector merely rotates to align, eventually with the deformation axis. This latter deformation is equivalent to the pseudo-affine deformation scheme described by Nobbs and Bower.[7]

The Helmholtz free energy of each chain at a given λ was calculated from $\ln P(\mathbf{r}_{def})$ resulting from the deformation of its end-to-end vector from $\mathbf{r}_0$ initially to $\mathbf{r}_{def}$ at λ. The total free energy for the network was evaluated as the sum of the free energies of the individual chains over the chains sampled. This procedure is distinct from approaches that use the uniform deformation of "average" chains.[8,9]

The normalized Helmholtz free energy change per chain for a network of ν chains can be expressed[3,4] in terms of the density, ρ, and the volume, V, of the (unswollen) network using

$$\frac{\Delta A}{\nu kT} = \frac{\Delta A}{RT\rho}\frac{M_c}{V} = \frac{1}{N}\sum_{i=1}^{N}(-\ln[P(r_{0,i})/P(r_{def,i})]) = s\left(\lambda^2 + \frac{2}{\lambda} - 3\right) \quad (4)$$

where R is the universal gas constant and M_c is the network chain molar mass. In general, s is a function of λ, although, for Gaussian network chains, $s = {}^1/_2$. Differentiation of eq 4 with respect to sample length, l, eventually yields[3,4] the normalized, true stress, $t/RT\rho$,

$$\frac{t}{RT\rho} = \frac{1}{nM_0}\left\{2s\left(\lambda^2 - \frac{1}{\lambda}\right) + (\lambda^3 - 3\lambda + 2)\frac{ds}{d\lambda}\right\} \quad (5)$$

M_0 is the average molar mass per skeletal bond, such that $M_c = nM_0$.

For the stress−optical calculations, the original network deformation algorithm[4] was enhanced[1] such that, for a given value of λ, concurrently with each chain deformation, the orientation function of the ith chain vector with respect to the applied strain, denoted $P_2(\psi_i)$, was calculated. Next, the value of $\langle P_2(\xi)\rangle_i$, for the average segment orientation with respect to the direction of the ith chain vector, was taken as equal to the value of $\langle P_2(\xi)\rangle$ at the value of r/r_{max} corresponding to the given λ for the particular chain. (The actual value of r/r_{max} corresponding to a given λ will vary, depending on the initial orientation of a chain.) In the event of a chain vector being extended beyond r^*_{max}, the magnitude of the deformed vector was set equal to r^*_{max}, thus defining the maximum value of $\langle P_2(\xi)\rangle_i$. However, as described previously, the direction of the chain vector was allowed to rotate from the direction defined by (x_0, y_0, z_0) to that which would be defined by the affinely deformed chain, irrespective of the magnitude of r.

For the M−C sample of N chains, the average chain vector orientation with respect to the deformation axis, $\langle P_2(\psi_i)\rangle$, the average segment orientation, $\langle\langle P_2(\xi)\rangle_i\rangle$, with

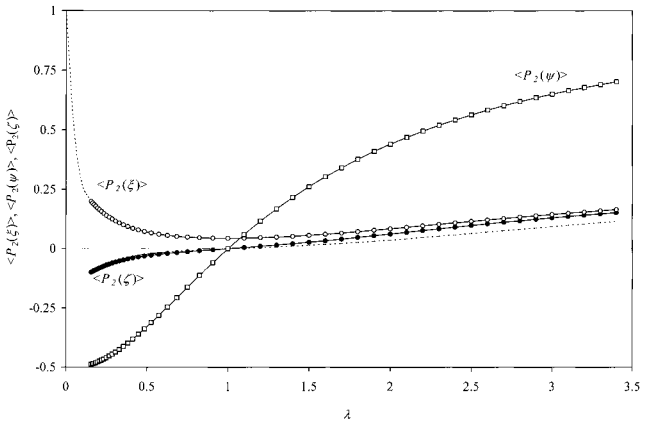

Figure 2. Average segmental orientation function components $\langle P_2(\xi)\rangle$, $\langle P_2(\psi)\rangle$, and $\langle P_2(\zeta)\rangle$ according to eq 1 (dashed curve) and eq 2 (continuous curve) for a 100-bond PE chain at 403 K.

respect to the end-to-end vector, and the average segment orientation with respect to the deformation axis, $\langle P_2(\zeta)\rangle$, are formed, as a function of λ, using

$$\langle P_2(\psi_i)\rangle = \frac{1}{N}\sum_{i=1}^{N} P_2(\psi_i) \tag{6}$$

$$\langle\langle P_2(\xi)\rangle_i\rangle = \frac{1}{N}\sum_{i=1}^{N}\langle P_2(\xi)\rangle_i \tag{7}$$

$$\langle P_2(\zeta)\rangle = \langle\langle P_2(\xi)\rangle_i P_2(\psi_i)\rangle = \frac{1}{N}\sum_{i=1}^{N}\langle P_2(\xi)\rangle_i P_2(\psi_i) \tag{8}$$

Equation 8 gives values of $\langle P_2(\zeta)\rangle$ corresponding to eq 2, whereas the product of $\langle\langle P_2(\xi)\rangle_i\rangle$ and $\langle P_2(\psi_i)\rangle$ defined by eqs 6 and 7 gives $\langle P_2(\zeta)\rangle$ corresponding to eq 1.

Results and Discussion

Deformation−Orientation Behavior. The values of $\langle P_2(\xi)\rangle$ and $\langle P_2(\psi)\rangle$ and of $\langle P_2(\zeta)\rangle$ according to eqs 1 and 2 for a network of 100-bond chains are plotted as functions of λ in Figure 2. The *nonzero* value of $\langle P_2(\xi)\rangle$ at $\lambda = 1$ was previously shown[1] to be characteristic of networks with *finite* network chain lengths. For the results calculated using eq 2, $\langle P_2(\zeta)\rangle$ moves closer to $\langle P_2(\xi)\rangle$ as extension increases and chain end-to-end vectors and segments tend to align parallel to each other. In contrast, the plots of $\langle P_2(\zeta)\rangle$ and $\langle P_2(\xi)\rangle$ from eq 1 remain parallel to each other as extension increases.

Calculated values of $\langle P_2(\zeta)\rangle$ for PE networks of chains of 40, 80, and 220 bonds at 403 K are plotted against $\lambda^2 - \lambda^{-1}$ in Figure 3. The values of $\langle P_2(\zeta)\rangle$ calculated using eq 2 become *considerably larger* as λ moves away from 1 than those calculated previously,[1] using eq 1, consistent with the behavior with respect to r/r_{max} shown in Figure 2. The plots now lie closer to the linear plots of the equivalent freely jointed, Gaussian chains. However, the Gaussian chains still overestimate the segmental orientation at the longer chain lengths ($n > 40$).

A closer look at the plots in Figure 3 in the extension region close to the origin ($\lambda \rightarrow 1$) reveals that, as expected, the *initial* slopes are not affected by the two averaging methods. This is shown in Figure 4 for extensional deformation, where values of $\langle P_2(\zeta)\rangle$ have been calculated in deformation steps of $\Delta\lambda = 0.01$, compared with $\Delta\lambda = 0.1$ used in the previous studies.[1,3]

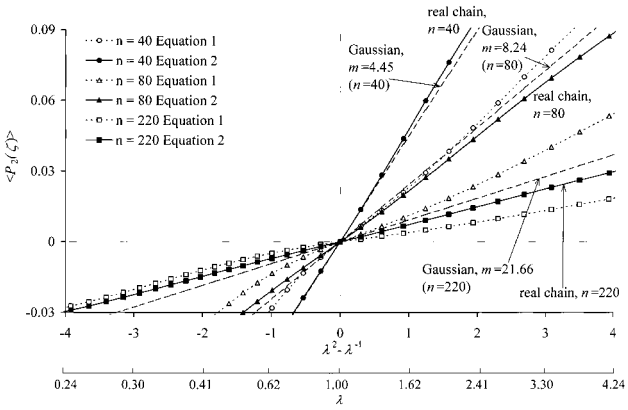

Figure 3. $\langle P_2(\zeta)\rangle$ calculated using eq 2 versus $\lambda^2 - \lambda^{-1}$ for networks of 40-, 80-, and 220-bond PE chains, at 403 K, and for Gaussian networks of freely jointed chains with number of links, $m = 4.45$ (conformationally equivalent[1] in $\langle r^2\rangle$ and r_{max} to $n = 40$), $m = 8.24$ (conformationally equivalent in $\langle r^2\rangle$ and r_{max} to $n = 80$), and $m = 21.66$ (conformationally equivalent in $\langle r^2\rangle$ and r_{max} to $n = 220$). Previous results, calculated using eq 1, are shown by dashed curves.

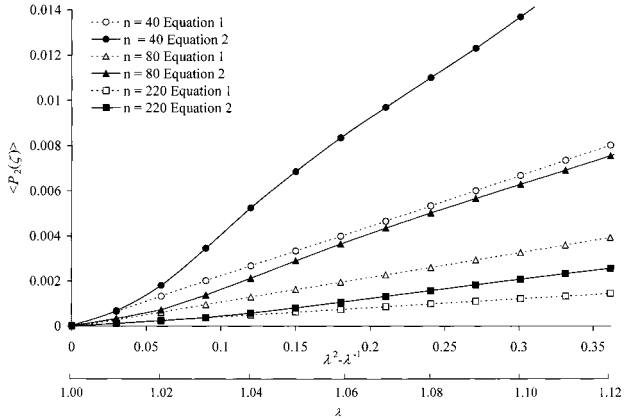

Figure 4. Values of $\langle P_2(\zeta)\rangle$ versus $\lambda^2 - \lambda^{-1}$, according to eqs 1 and 2, for networks of 40-, 80-, and 220-bond PE chains at 403 K in extension, in the region $\lambda \rightarrow 1$. $\langle P_2(\zeta)\rangle$ was evaluated in steps of $\Delta\lambda = 0.01$.

It can be seen that as $\lambda \rightarrow 1$, the values of $\langle P_2(\zeta)\rangle$ from the two averaging methods become indistinguishable, because chain vectors in the undeformed network are randomly oriented with respect to the strain axis[1] and all values of ξ occur randomly with all values of ψ. As λ increases, the independence of ξ and ψ is rapidly lost. Overall, from Figures 3 and 4, the shape of the $\langle P_2(\zeta)\rangle$ versus $\lambda^2 - \lambda^{-1}$ plots, with $\langle P_2(\zeta)\rangle$ evaluated using eq 2, is seen to be sigmoidal. However, in the range of λ shown in Figure 4, $\langle P_2(\zeta)\rangle$ evaluated using eq 1 is linear in $\lambda^2 - \lambda^{-1}$ and, as seen from Figure 3, is nonlinear at higher values of λ. The linearity at λ near 1 is expected because ψ and ξ are independent and chains are deforming affinely, as in the conventional treatment of freely jointed chains.[8] As λ increases, some chains reach full extension and give rise to the curvature shown in the plots in Figure 3.

The deformation−orientation coefficient, Z_λ, is defined[1] by the equation

$$\langle P_2(\zeta)\rangle = Z_\lambda(\lambda^2 - \lambda^{-1}) \tag{9}$$

Figure 5 shows the variation of Z_λ as a function of $\Delta\lambda$, with Z_λ evaluated assuming $\langle P_2(\zeta)\rangle$ and $\lambda^2 - \lambda^{-1}$ are directly proportional to each other between $\lambda = 1 + \Delta\lambda$.

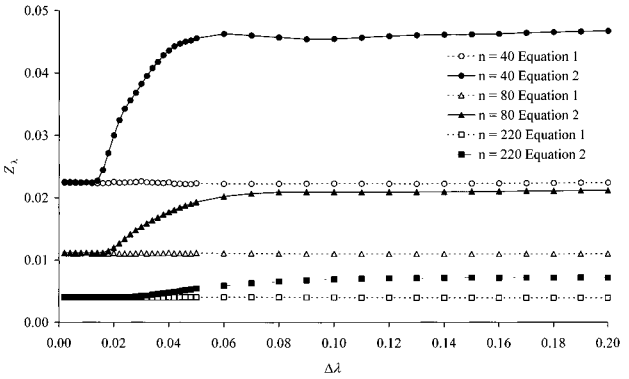

Figure 5. Calculated values of Z_λ versus $\Delta\lambda$ for networks of 40-, 80-, and 220-bond PE chains. Values based on eq 1 are represented by the closed symbols, and those based on eq 2 are represented by the open symbols.

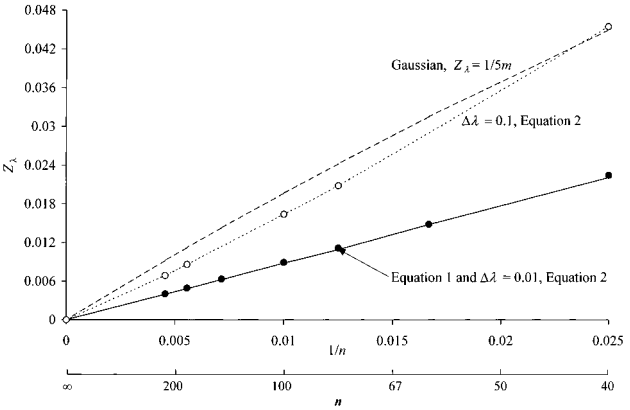

Figure 6. Calculated values of Z_λ versus $1/n$ for PE networks at 403 K. The ● symbols denote the values of $\langle P_2(\zeta)\rangle$ averaging based on eq 2 and using a deformation step $\Delta\lambda = 0.01$. The continuous line shows the previous[1] Z_λ values evaluated according to eq 1. The effect of using a larger step size, of $\Delta\lambda = 0.1$, with eq 2, is also shown, together with the values of Z_λ ($= 1/5m$) for equivalent freely jointed chains of m links (dashed curve).

In other words, Z_λ has been evaluated from the plots in Figure 4 by drawing straight lines from the origin to the points on the curves corresponding to $\lambda = 1 + \Delta\lambda$. For $\Delta\lambda \leq 0.01$, the values of Z_λ based on both eqs 1 and 2 are essentially the same for a given chain length. For $\Delta\lambda > 0.01$ the value of Z_λ based on eq 2 changes as $\Delta\lambda$ increases and tends toward higher values, which remain *approximately* constant. The increase in Z_λ is seen to become more gradual as chain length increases. For Z_λ based on eq 1 it can be seen that, corresponding to the linear behavior shown in Figure 4, there is no sensitivity to $\Delta\lambda$ over the range of $\Delta\lambda$ values shown. Importantly, if a sufficiently small deformation step ($\Delta\lambda \leq 0.01$, approximately) is used, the *initial* slopes of the plots in Figure 4, defining Z_λ, are not affected by the method of averaging used to form $\langle P_2(\zeta)\rangle$.

Values of Z_λ, evaluated at $\Delta\lambda = 0.01$ and $\Delta\lambda = 0.1$, are plotted as a function of the reciprocal number of skeletal bonds, $1/n$, in Figure 6. The values for $\Delta\lambda = 0.1$ are taken as "typical" of those for $0.06 \geq \Delta\lambda \geq 0.20$. As one would expect from Figure 5, it can be seen that the values of Z_λ based on eq 2 and, using the values of $\langle P_2(\zeta)\rangle$ and $(\lambda^2 - \lambda^{-1})$ at $\lambda = 1$ and $\lambda = 1.01$, i.e., $\Delta\lambda = 0.01$ (shown by the filled circles), are indistinguishable from those calculated previously,[1] using eq 1 (shown by the continuous line). However, if the correct averaging of eq 2 is used and the deformation step size is

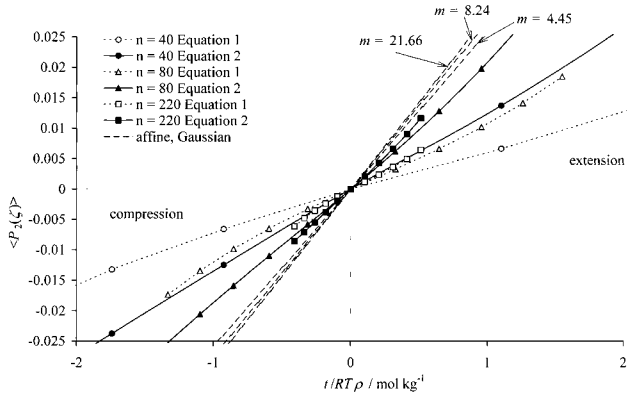

Figure 7. $\langle P_2(\zeta)\rangle$ versus normalized true stress, $t/RT\rho$, for PE networks with $n = 40$, 80, and 220 bonds at 403 K. The corresponding plots for networks of Gaussian chains with $m = 4.45$, 8.24, and 21.66 (equivalent to PE chains with $n = 40$, 80, and 220, respectively) are also shown.

increased, the calculated values of Z_λ (shown by the open circles) will be misleadingly increased, coincidentally, nearer to Gaussian values, given by the equation[1]

$$Z_\lambda = \frac{1}{5m} \tag{10}$$

where m is the number of freely jointed links equivalent to n real skeletal bonds. Hence, with regard to comparisons between theory and experimental behavior on the basis of eq 9 and a constant value of Z_λ, it appears that *accurate* determinations of Z_λ at small deformation ratios are needed (see Figure 5). Such ratios, $\lambda \leq 1.01-1.03$, depending on chain length, are somewhat smaller than those normally employed experimentally.

Stress−Orientation Behavior. The effects of using the values of $\langle P_2(\zeta)\rangle$ from eq 2 on the stress−orientation behavior are shown in Figure 7. Again, points are plotted corresponding to intervals of 0.1 in $\Delta\lambda$, and the differences in the results from the two methods of averaging are significant. Equation 2 gives higher values of $\langle P_2(\zeta)\rangle$ that lie nearer to those from the Gaussian approximation. However, the Gaussian approximation still gives values of orientation that are too high and do not show a large enough chain length dependence.

Again, using a deformation step size of $\Delta\lambda = 0.01$, the stress−orientation behavior for networks of 40- and 220-bond PE chains are plotted in Figure 8. (The results for 80 bonds have been omitted for clarity.) Near the origin, the plots for a given chain length, using the two averaging procedures, are indistinguishable. As macroscopic deformation increases, the larger values of $\langle P_2(\zeta)\rangle$ at a given r/r_{max}, resulting from the correct averaging procedure of eq 2, give increases in the stress−orientation relative to that calculated from eq 1. Also, more marked nonlinear behavior is observed.

The initial slopes of the plots in Figures 7 and 8 are equal to the stress−orientation coefficient, Z_t.

$$Z_t = \left[\frac{\langle P_2(\zeta)\rangle \rho RT}{t}\right]_{\lambda \to 1} \tag{11}$$

ρ is the network density and t the true stress. As with Z_λ, if linear behavior over the different ranges of $\Delta\lambda$, near $\lambda = 1$, is assumed, then different values of Z_t result. Accordingly, Figure 9 shows the variation of Z_t as a function of $\Delta\lambda$. For $\Delta\lambda \leq 0.01$, the values of Z_t based on

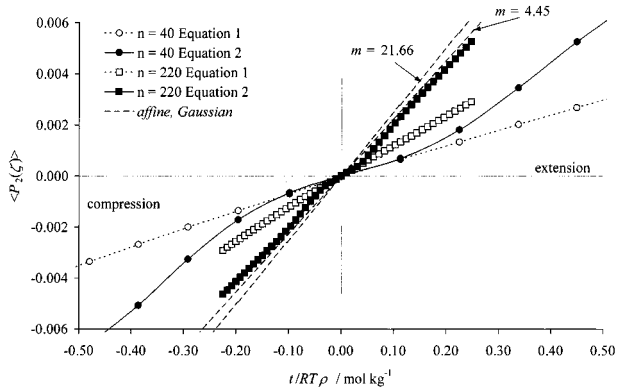

Figure 8. $\langle P_2(\zeta)\rangle$ versus normalized true stress, $t/RT\rho$, for the networks of 40- and 220-bond PE chains at 403 K at macroscopic extensions in the region $\lambda \rightarrow 1$, using a deformation step $\Delta\lambda = 0.01$. The plots for Gaussian networks with $m = 4.45$ and $m = 21.66$ are also shown.

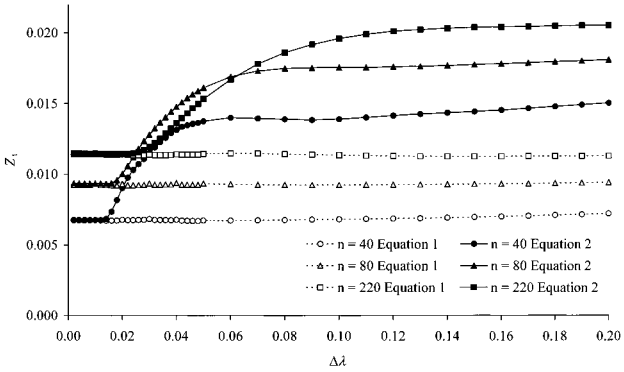

Figure 9. Calculated values of Z_t versus $\Delta\lambda$ for networks of 40-, 80-, and 220-bond PE chains. Values based on eq 1 are represented by the open symbols, and those based on eq 2 are represented by the closed symbols.

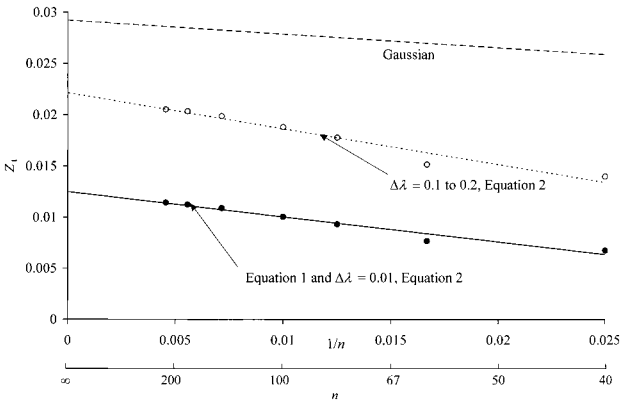

Figure 10. Stress−orientation coefficient, Z_t, as a function of reciprocal number of skeletal bonds, $1/n$, for PE networks at 403 K. Values of Z_t determined from $t/RT\rho$ and $\langle P_2(\zeta)\rangle$ data defined at deformation steps of $\Delta\lambda = 0.01$ and 0.1 using eqs 2 and 1. The Gaussian curve follows eq 12.

both eqs 1 and 2 are the same for all the chain lengths shown. For $\Delta\lambda > 0.01$, the values of Z_t based on eq 2 increase rapidly as $\Delta\lambda$ increases, toward approximately constant values. For Z_t based on eq 1 it can be seen that there is no sensitivity to $\Delta\lambda$ over the range of $\Delta\lambda$ shown (cf. Figure 5)

Values of Z_t are plotted as a function of $1/n$ in Figure 10, and it can be seen that if *initial* slopes of the plots using eq 2 and $\Delta\lambda = 0.01$ are compared with those using eq 1, the differences in Z_t introduced by the two methods of averaging are negligible, as expected. However, if eq 2 is used and the deformation step size is increased to $\Delta\lambda = 0.1-0.2$, the calculated values of Z_t will be misleadingly increased.

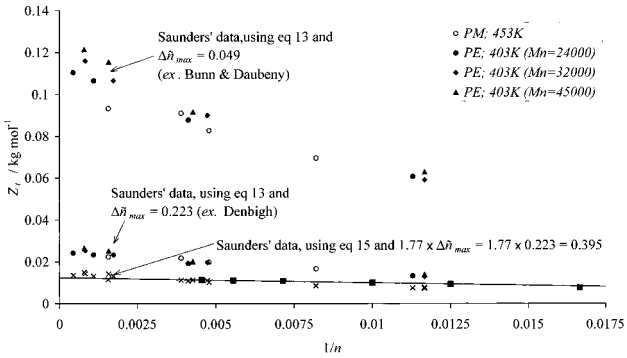

Figure 11. Z_t versus $1/n$ calculated for model networks of 40-bond to 220-bond PE chains (■), compared with values of Z_t derived from Saunders' experimental values of the stress−optical coefficient using eq 13 with $\Delta\tilde{n}_{max} = 0.049$ (Bunn and Daubeny[12]) and $\Delta\tilde{n}_{max} = 0.223$ (Denbigh[11]) and eq 15 with $1.77 \times \Delta\tilde{n}_{max} = 1.77 \times 0.223 = 0.395$ (compare Figure 12 of ref 1).

The Gaussian values of Z_t shown in Figure 10 are given by[1]

$$Z_t = \frac{M_c}{5m} = \frac{M_0}{5}\,\frac{n}{m} \tag{12}$$

where M_c is the molar mass of the network chains of m equivalent links or n skeletal bonds, with M_0 the molar mass per skeletal bond. They are much larger than *either* M−C estimate and have a weaker dependence on $1/n$, the dependence coming from the variation of n/m with chain length.

Comparison with Experimental Stress−Optical Behavior. Limiting stress−optical behavior for small deformations and its characteristic parameters are unaffected by which method of averaging is used to evaluate $\langle P_2(\zeta)\rangle$. Thus, the values of deformation−orientation coefficient (Z_λ) and stress−orientation coefficient (Z_t) evaluated previously (cf. Figures 6 and 10 of the present paper with Figures 8 and 11 of ref 1) are still correct. However, the nonlinear behaviors of $\langle P_2(\zeta)\rangle$ versus $\lambda^2 - \lambda^{-1}$ and $t/RT\rho$ (see Figures 4 and 9) mean that *experimental* determinations of the stress−optical coefficients and deduced values of Z_λ and Z_t may be significantly in error if $\lambda \geq 1.02$, approximately, is the smallest deformation used experimentally. In Figure 10, as $n \rightarrow \infty$, the ratio of the values of Z_t evaluated from eq 2 with $\Delta\lambda = 0.1-0.2$ to those evaluated with $\Delta\lambda = 0.01$ is found to be equal to $(0.0221/0.0125) = 1.77$.

Experimentally, Z_t is conventionally evaluated from the measured stress−optical coefficient (C) using the equation

$$Z_t = \frac{C\rho RT}{\Delta\tilde{n}_{max}} \tag{13}$$

where $\Delta\tilde{n}_{max}$ is the maximum possible birefringence with all segments aligned with the macroscopic strain direction. C is formally evaluated as

$$C = \left[\frac{\Delta\tilde{n}}{t}\right]_{\lambda\rightarrow 1} \tag{14}$$

where $\Delta\tilde{n}$ is the observed birefringence. The results of Saunders[10] for polyethylene previously fitted,[1] as shown

in Figure 11, came from *linear* birefringence ($\Delta\tilde{n}$) versus stress (t) plots and corresponded to $1.1 \geq \lambda \geq 1.05$ as the *smallest* deformation. Hence, from Figure 10, the values of Z_t deduced from experimental values of C, C_{expt} (corresponding to linear behavior of $\langle P_2(\zeta)\rangle$ versus $t/RT\rho$ up to $\lambda = 1.1-1.2$, viz., $\Delta\lambda = 0.1-0.2$), will be 1.77 times larger than the true limiting values as $\lambda \rightarrow 1$. That is, the true value of Z_t is given by

$$Z_t = \frac{C_{expt}\rho RT}{1.77\Delta\tilde{n}_{max}} \tag{15}$$

Thus, in Figure 11, agreement between experiment and theory is achieved using a value of $\Delta\tilde{n}_{max}$ of 0.223, calculated using Denbigh's[11] polarizabilities based on data for gaseous CH_4 and C_2H_6, with

$$Z_t = \frac{C_{expt}\rho RT}{1.77 \times 0.223} = \frac{C_{expt}\rho RT}{0.395} \tag{16}$$

As discussed in our previous paper,[1] the value of $\Delta\tilde{n}_{max}$ of 0.223 compares with a value of 0.049 calculated on the basis of Bunn and Daubeny's[12] experimental measurements of paraffin crystals. The results obtained for Z_t using $\Delta\tilde{n}_{max} = 0.049$ are also shown in Figure 11.

Conclusions

Correction of the averaging procedure used to evaluate the segmental orientation function, $\langle P_2(\zeta)\rangle$ of polyethylene network chains, shows that it is linearly related to $\lambda^2 - \lambda^{-1}$ and to normalized stress $t/RT\rho$ only at $\lambda \approx 1$. Marked deviations from linearity rapidly occur as segments become noticeably nonrandomly oriented at relatively small deformations. Assuming linear behavior between $\langle P_2(\zeta)\rangle$ and $\lambda^2 - \lambda^{-1}$ and $t/RT\rho$, the derived deformation−orientation and stress−orientation coefficients, Z_λ and Z_t, are very different when evaluated at 1% strain compared with 10−20% strain, and the average values at the latter levels of strain are more likely to correspond to those determined experimentally. With respect to Z_t, this means that experimental values for polyethylene are 1.77 times the values calculated at 1% strain, and agreement between calculation and experiment can be achieved using Denbigh's values for the bond polarizabilities of the structural unit. Analytical calculations by Brereton and Ries[13] based on the freely jointed chain show a value of Z_t in the range between 1.7 and 1.8 times the numerical limiting value as $\lambda \rightarrow 1$. However, there are differences between the analytical and numerical values of Z_t at $\lambda = 1$ that still need to be resolved.[13] It is expected that nonlinear stress−orientation behavior near $\lambda = 1$ will be a general phenomenon for all chain structures and needs to be taken account of when comparing experimental measurements and theoretical predictions of Z_λ and Z_t.

Acknowledgment. Support of the EPSRC (Grants GR/L/66649 and GR/L/62306) is gratefully acknowledged.

References and Notes

(1) Taylor, D. J. R.; Stepto, R. F. T.; Jones, R. A.; Ward, I. M. *Macromolecules* **1999**, *32*, 1978.
(2) Abe, A.; Jernigan, R. L.; Flory, P. J. *J. Am. Chem. Soc.* **1966**, *88*, 631.
(3) Stepto, R. F. T.; Taylor, D. J. R. *Macromol. Symp.* **1995**, *93*, 261.
(4) Stepto, R. F. T.; Taylor, D. J. R. *J. Chem. Soc., Faraday Trans.* **1995**, *91*, 2639.
(5) Flory, P. J. *Statistical Mechanics of Chain Molecules*; Interscience: New York, 1969.
(6) Mattice, W. L.; Suter, U. W. *Conformational Theory of Large Molecules*; John Wiley & Sons Inc.: New York, 1994.
(7) Nobbs, J. H.; Bower, D. I. *Polymer* **1978**, *19*, 1100.
(8) Treloar, L. R. G. *The Physics of Rubber Elasticity*, 3rd ed.; Clarendon Press: Oxford, 1975.
(9) Flory, P. J.; Erman, B. *Macromolecules* **1983**, *16*, 1601, 1607.
(10) Saunders, D. W. *Trans. Faraday Soc.* **1954**, *50*, 881.
(11) Denbigh, K. G. *Trans. Faraday Soc.* **1940**, *36*, 936.
(12) Bunn, C. W.; Daubeny, R. de P. *Trans. Faraday Soc.* **1954**, *50*, 1173.
(13) Brereton, M. G.; Ries, M. E., to be published.

MA991943N